

Ultrathin limit and dead-layer effects in local polarization switching of BiFeO₃

Peter Maksymovych,^{1,*} Mark Huijben,^{2,3} Minghu Pan,¹ Stephen Jesse,¹ Nina Balke,¹ Ying-Hao Chu,⁴ Hye Jung Chang,⁵ Albina Y. Borisevich,⁵ Arthur P. Baddorf,¹ Guus Rijnders,² Dave H. A. Blank,² Ramamoorthy Ramesh,³ and Sergei V. Kalinin¹

¹Center for Nanophase Materials Sciences, Oak Ridge National Laboratory, Oak Ridge, Tennessee 37831, USA

²Faculty of Science and Technology, MESA + Institute for Nanotechnology, University of Twente, P.O. Box 217, 7500 AE Enschede, The Netherlands

³Department of Materials Sciences and Engineering and Department of Physics, University of California–Berkeley, Berkeley, California 94720, USA

⁴Department of Materials Science and Engineering, National Chiao Tung University, HsinChu 30010, Taiwan

⁵Materials Science and Technology Division, Oak Ridge National Laboratory, Oak Ridge, Tennessee 37831, USA

(Received 28 January 2011; revised manuscript received 23 September 2011; published 31 January 2012)

Using piezoresponse force microscopy in an ultrahigh vacuum, polarization switching has been detected and quantified in epitaxial BiFeO₃ films from 200 to about 4 unit cells thick. Local remnant piezoresponse was utilized to probe both ferroelectric properties and effects of imperfect electrical contacts. It was found that the shape of electromechanical hysteresis loops is strongly influenced by an extrinsic dielectric gap, primarily through the suppressing effect of the depolarizing field on the spontaneous polarization in the ultrathin films. Furthermore, statistical analysis of the hysteresis loops has revealed lateral variation of the extrinsic dielectric gap with sub-10-nm resolution. Robust and reproducible ferroelectric properties of nanoscale BiFeO₃ indicate its potential for nanoscale applications in information storage and spintronics.

DOI: [10.1103/PhysRevB.85.014119](https://doi.org/10.1103/PhysRevB.85.014119)

PACS number(s): 77.80.Fm, 68.37.–d, 77.65.–j, 77.80.Dj

I. INTRODUCTION

Ferroelectric materials and polarization switching in confined geometries have strong potential for information storage,^{1,2} energy storage,³ optoelectronic and spintronic applications.^{4,5} Ferroelectricity also is subject to pronounced size effects, manifested as scaling of the magnitude of ferroelectric polarization^{6,7} and scaling of the coercive field that triggers polarization switching,^{8–11} as well as the evolution of the polarization domain morphology with the size^{12,13} and dimensionality^{14,15} of ferroelectric and multiferroic materials. Although ferroelectric size effects have been investigated for many decades,^{16,17} many questions remain open or controversial.

One such question, which pertains to many prospective ferroelectric applications, relates to the scaling of the coercive field (E_c) with film thickness (h) or dimensionality. For macroscopic films, with dimensions far exceeding the correlation length, the coercive field follows the Kay-Dunn law $E_c \sim h^{-2/3}$,¹⁸ established using the Landauer nucleation model for polarization switching.¹⁹ In the original model, the Kay-Dunn law is expected to break down at an ultrathin limit, because the nucleus shape changes from the half-prolate Landauer shape¹⁹ to a cylindrical shape, which in turn cancels the depolarizing energy of the charged apex. In this case, the coercive field scaling is expected to saturate at a certain value. While this scenario was invoked by Jo *et al.*⁸ to explain the saturation of the field in epitaxial BaTiO₃/SrRuO₃ capacitors below ~ 10 nm, other authors, based on studies of the ferroelectric polymer polyvinylidene fluoride (PVDF),¹⁰ have claimed that the saturation signals the onset of intrinsic ferroelectric switching, where the direction of spontaneous polarization is reversed uniformly throughout the film rather than through the nucleation-growth mechanism. Finally, Dawber *et al.*¹¹ suggested that Kay-Dunn scaling in PVDF switching should be recovered

down to as low as 1 nm by including the effect of the dielectric dead layer and the depolarizing field in the polymer film.

Reliable interpretation of size-dependent ferroelectric switching requires the knowledge of the electric field inside the ferroelectric volume. However, the electric field is in general nonuniform throughout the ferroelectric capacitor because of dead layers (manifested, among other effects, as dielectric gaps in the contact region), dopant profiles, and space-charge regions, the properties of which are largely unknown. The problem is further complicated because conventional polarization–electric field (P-E) hysteresis measurements based on the displacement current are not explicitly sensitive to dielectric gaps.²⁰ The resulting uncertainty in the interpretation becomes most pronounced at the ultrathin limit, where extrinsic effects dominate the electric field profile.

Here, we studied the properties of ferroelectric switching in ultrathin films using the magnitude and hysteresis of piezoresponse (strain due to applied electric field),²¹ rather than those of the displacement current, as in conventional P-E measurements. Under a reasonable assumption that the overall piezoresponse is dominated by the ferroelectric volume, the magnitude of piezoresponse provides a direct measure of the electric field inside the ferroelectric. Systematic analysis of piezoresponse hysteresis loops allowed us to detect remnant and switchable polarization down to 4 unit cells (1.6 nm) in epitaxial films of BiFeO₃ (BFO) and infer the presence of the dielectric gaps and the intrinsic ferroelectric behavior. Furthermore, we have, for the first time, spatially resolved the variation of the dielectric gap effects with < 10 -nm resolution.

II. EXPERIMENTAL DETAILS

BFO films were deposited on 5-nm conducting La_{0.7}Sr_{0.3}MnO₃ (LSMO) electrodes by pulsed-laser deposi-

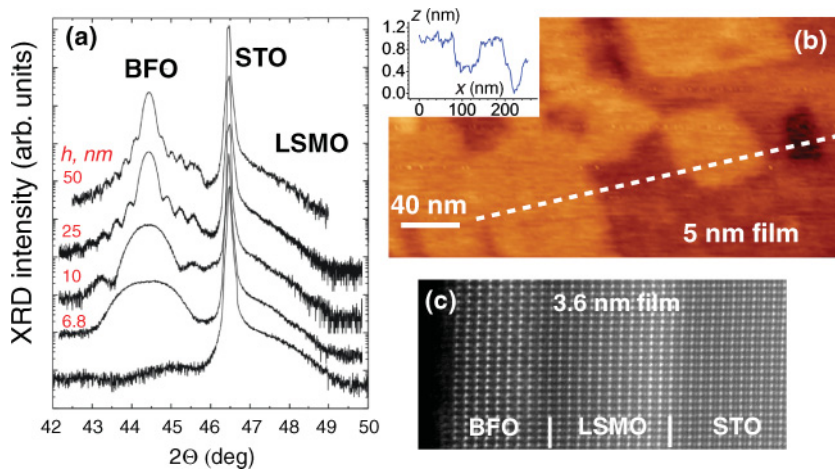


FIG. 1. (Color online) (a) X-ray diffraction analysis of BFO(100)/LSMO films, some of which were subsequently used in PFM measurements. The thickness of LSMO is 5 nm for all BFO films. Scans are shifted for clarity. (b) AFM topography of the 5-nm BFO film and its cross section (inset) along the white dashed line. (c) Z-contrast scanning transmission electron microscopy image of a cross-section of a 3.6 nm BFO film.

tion (PLD) with reflection high-energy electron diffraction (RHEED) control of the growth process, at 750 °C and $P_{O_2} = 200$ mTorr for LSMO and 670 °C and $P_{O_2} = 100$ mTorr for BFO.^{22,23} After the growth, the heterostructures were slowly cooled to room temperature in 1 atm of oxygen at a rate of ~ 5 K/min. Film thicknesses were determined from RHEED analysis during PLD growth and independently confirmed by transmission electron microscopy and x-ray ellipsometry on representative samples. BFO films (except 12 and 50 nm) were first annealed at ~ 350 °C and $P_{O_2} = 10$ mTorr to remove surface contamination, while preventing film decomposition and changes of stoichiometry (described later), and then introduced into the vacuum microscope chamber without exposure to ambient. The high crystalline quality of the films was supported by x-ray diffraction [Fig. 1(a)], atomic force microscopy exhibiting flat topography with unit-cell high steps (as seen in Fig. 1(c) for a representative 5-nm film), and scanning transmission electron microscopy [Fig. 1(c)].

Piezoelectric and ferroelectric properties were characterized using piezoresponse force microscopy (PFM) in an ultra-high vacuum at the background pressure of $\sim 2 \times 10^{-10}$ Torr as described elsewhere.²⁴ Local piezoresponse hysteresis loops were acquired by applying bias pulses of increasing magnitude to the tip (Pt-coated Mikromasch CSC37) and measuring the out-of-plane remnant piezoresponse between the pulses. Although we did not directly control the size and curvature of the probe tip, which determines the spatial distribution and strength of applied electric field, we estimated it to be much larger (> 25 nm) than the thickness of the ultrathin films (except for the 50-nm film), and we did not detect any significant difference in the switching behavior obtained with different tips.

The measurement sensitivity was maximized using the band-excitation technique,²⁵ where the cantilever is excited by a band of frequencies in the vicinity of the first contact resonance [Fig. 2(a) and 2(b)]. Fig. 2(a) shows a typical hysteresis measurement on a 2.8-nm BFO film and the hysteresis loops [Fig. 2(c)] extracted by integrating the response in the probed frequency range.

III. RESULTS

A. Average thickness dependence of local ferroelectric switching

Although the PFM methodology was applied to ultrathin BFO and $PbTiO_3$ films, as well as nanoparticles, in previous works,^{7,22,27–30} all such measurements were carried out in an ambient environment and thus could be compromised by extrinsic local electrochemical reactions, particularly in the thickness range of < 10 nm, as previously noted for BFO²² and other perovskite surfaces.³¹ Furthermore, only in-field piezoresponse^{22,30} was used to infer ferroelectric switching in ultrathin films, leaving uncertain the existence of switchable remnant polarization and the respective size effects.

Here, the piezoresponse hysteresis loops corresponding to the switching of remnant out-of-plane polarization were reproducibly observed down to the thinnest, 1.6-nm BFO film [Fig. 3(a)]. The hysteresis loops on two separate 2-nm films, only one of which had been annealed in vacuum, were nearly identical [Fig. 3(b)], indicating that the measured properties were intrinsic to as-grown films. Good reproducibility of the hysteresis loops in consecutive switching cycles [Figs. 2(a) and 2(c)] and negligible variation of the contact resonance frequency during ferroelectric switching [Fig. 2(d)] testified to the lack of surface damage and electrochemical reactions during ferroelectric switching. At the same time, we verified that spontaneous polarization of the 2-nm [Figs. 3(c) and 3(d)] and 5-nm (not shown) BFO films could be reversed in a large surface area ($\sim 90 \times 140$ nm² for the 2-nm film) by poling it with a biased tip. Altogether, we conclude that epitaxial BFO retains ferroelectricity down to at least 1.6 nm.

Comparative statistics for the thickness dependence of ferroelectric switching was derived from 30 to 100 hysteresis loops from each film. Each hysteresis loop was fitted with a phenomenological function [Fig. 2(c)] to extract the switching bias.²⁵ The average hysteresis loops [Fig. 3(a)] revealed rapid drop-off of remnant piezoresponse with decreasing film thickness [Fig. 3(b)], as well as significant lowering of the switching bias. Given the imperfections in the chemical stoichiometry found at the interfaces of epitaxial oxide films, as well as the nonepitaxial top contact (tip–surface), it is

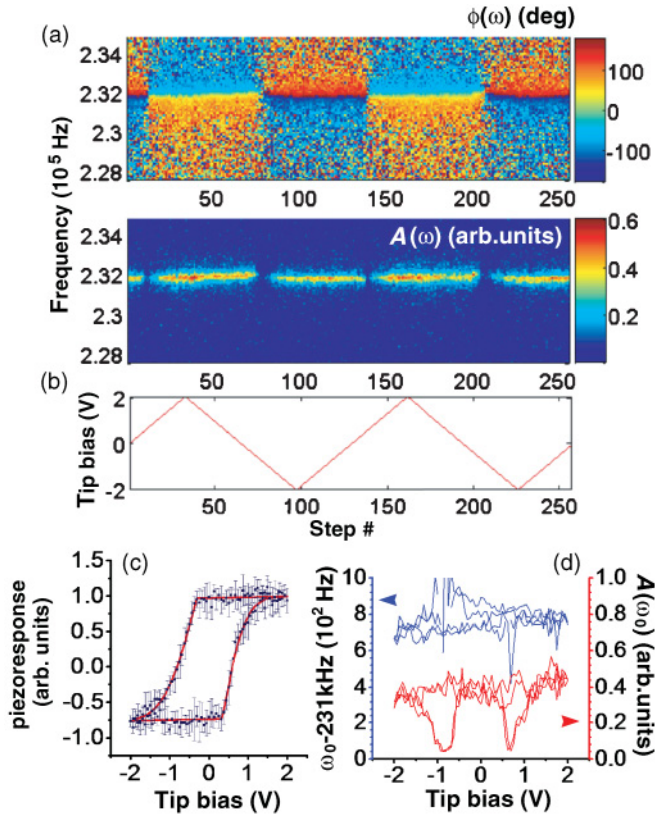


FIG. 2. (Color online) (a) Band-excitation piezoresponse force spectroscopy of two consecutive cycles of the ferroelectric switching on the surface of a 2.8-nm BFO film in ultrahigh vacuum. Pseudocolor plots show the frequency spectrum of the amplitude and phase of cantilever oscillation at its first contact resonance frequency (~ 232 kHz) along (b) the bias trajectory of ferroelectric switching. (b) The envelope of tip bias used to locally switch ferroelectric polarization. (c) Average hysteresis loop extracted from (a) and (b) as described in the text. The red (medium gray) lines show a fit using a phenomenological function. (d) Resonance frequency and resonant amplitude of cantilever oscillation along the ferroelectric hysteresis loop.

reasonable to assume the existence of the dielectric gaps within the Pt-tip–BFO–LSMO nanocapacitor, which lower the electric field inside the BFO film compared to the perfect-contact scenario¹¹ and could explain the observed trend. In this case, the normal component of the electric field inside the film E_z can be approximated by a capacitor model with dielectric gaps²⁰

$$E_z = \frac{U \varepsilon_d}{\varepsilon_d h + \varepsilon_h^b d} - \frac{P_z d}{\varepsilon_0 (\varepsilon_d h + \varepsilon_h^b d)}, \quad (1)$$

where d is the total thickness of the dielectric gaps, U is the potential across the film, P_z is the out-of-plane polarization component, ε_d is the dielectric constant of the dead layer (assumed the same for top and bottom layers), and ε_h^b is the dielectric background constant of the ferroelectric/piezoelectric volume, i.e., independent of the film thickness, in contrast to the dielectric permittivity ε_{33}^f part related to the soft mode.

The thickness of the dielectric gaps d is not known *a priori*, presenting a major problem for the quantitative in-

terpretation of the ferroelectric hysteresis loops from ultrathin films (particularly the thickness dependence of the switching voltage), obtained both locally as in our experiments and in capacitor measurements with fixed electrodes. However, local piezoresponse is a second independent observable value, which can potentially provide the much-needed information on the scaling of the electric field profile and/or polarization across the thickness range or across the surface of the ferroelectric film.

Assuming uniform polarization perpendicular to the film's surface, the out-of-plane piezoelectric strain produced in the tetragonal film by applied electric field can be expressed as $u_z \propto h \cdot E_z \varepsilon_{33} \varepsilon_0 Q_{11} P_z$, where E_z is the electric field inside the ferroelectric and ε_{33} and Q_{11} are the components of the dielectric and electrostrictive tensors, respectively. Experimentally, the out-of-plane piezoresponse is measured approximately as a first derivative of the out-of-plane piezoelectric strain with respect to applied bias, $\partial u_z / \partial U$. Thus, if we were to assume a linear potential drop across the whole Pt-tip/BFO/LSMO structure (a perfect-contact scenario) with a corresponding out-of-plane electric field component of $E_z = U/h$, the measured piezoresponse would depend only on the magnitude of spontaneous polarization P_z . The dielectric gaps located at the interfaces (1) lower the electric field inside the ferroelectric volume of Eq. (1) and (2) suppress the magnitude of spontaneous polarization because of the depolarizing field, the second term in Eq. (1). Therefore, in the presence of the dielectric gaps, both pure electrostatics of the junction and the scaling of the ferroelectric properties of the film contribute to the overall thickness dependence of piezoresponse (more generally, intrinsic scaling of the dielectric properties and the polarization also contribute to the thickness dependence of piezoresponse). To analyze this problem further, we first introduce the relevant aspects of the intrinsic model for ferroelectric switching²⁶ in the context of finite film thickness and interfacial dielectric gaps. Our previous experiments^{24,32} have shown that intrinsic switching is the dominant mechanism for polarization reversal in PFM measurements.

B. Model for thickness dependence of intrinsic switching

The one-dimensional (1D) model detailed here is applicable while $h \ll R$, i.e., for film thickness h smaller than the tip radius R . Because $R > 25$ nm (see the Appendix) the model can be applied to all studied BFO films, with a possible exception of the 50-nm film. The presence of the thickness-dependent depolarization field self-consistently reduces the polarization value P_z via the ferroelectric equation of state with cubic nonlinearity:²⁶

$$\alpha \langle P_z \rangle + \beta \langle P_z^3 \rangle = \langle E_z \rangle + E_b. \quad (2)$$

Here, we use the average polarization $\langle P_3 \rangle \equiv \frac{1}{h} \int_0^h P_3(\tilde{z}) d\tilde{z}$. The built-in field E_b is proportional to the built-in potential and polarization contributions: $E_b = \frac{\varepsilon_d U_b}{\varepsilon_d h + \varepsilon_h^b d} - \frac{P_b}{\varepsilon_0 \varepsilon_h^b}$. Then, Eq. (2) can be rewritten, including the renormalized coefficient $\alpha_R = \alpha + \frac{1}{\varepsilon_0} \frac{d}{\varepsilon_d h + \varepsilon_h^b d}$, as

$$\alpha_R \langle P_z \rangle + \beta \langle P_z^3 \rangle = \frac{U \varepsilon_d}{\varepsilon_d h + \varepsilon_h^b d} + E_b. \quad (3)$$

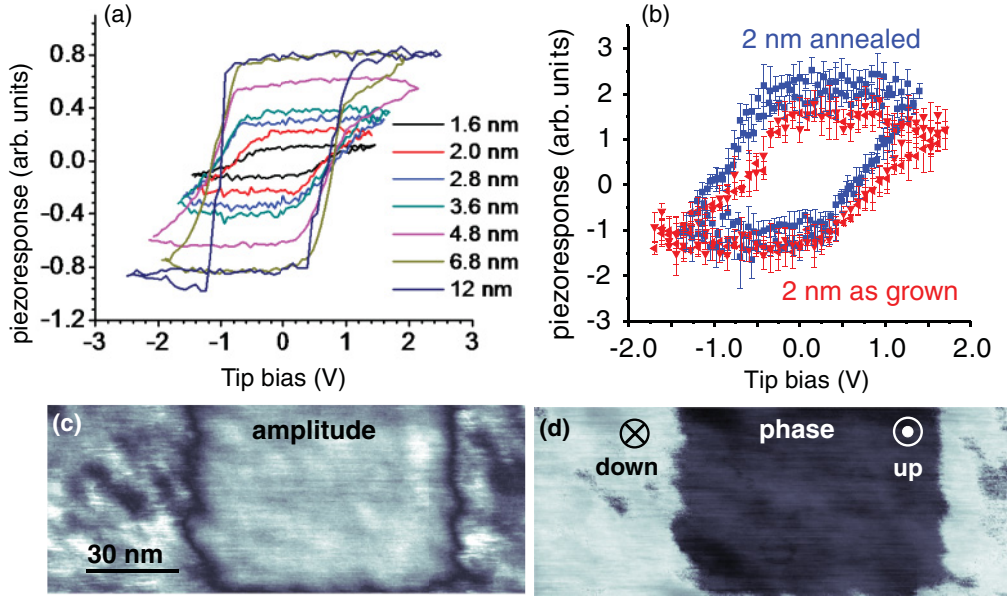


FIG. 3. (Color online) Average hysteresis loops acquired from 10 to 30 random locations on the surfaces of BFO films ranging from 1.6 to 12 nm. The loops were acquired using the same physical cantilever in ultrahigh vacuum. (b) Comparison of vacuum piezoresponse hysteresis loops from two 2-nm BFO/LSMO films, only one of which was annealed in vacuum. (c) Piezoresponse amplitude and (d) phase of an upward-polarized ferroelectric domain recorded on the 2-nm film by poling the area in the center at -0.8 V.

Then thermodynamic or intrinsic coercive bias becomes

$$\begin{aligned}
 E_c^b &= -E_b \pm \frac{2}{3\sqrt{3}} \sqrt{-\frac{\alpha_R^3}{\beta}} \\
 &= -E_b \pm E_c^0 \left(1 + \frac{1}{\alpha \varepsilon_0} \frac{d}{\varepsilon_d h + \varepsilon_h^b d}\right)^{3/2} \\
 &\stackrel{\varepsilon_d h \gg \varepsilon_h^b d}{\approx} -E_b \pm E_c^0 \left(1 + \frac{1}{\alpha \varepsilon_0} \frac{d}{\varepsilon_d h}\right)^{3/2} \\
 &\sim E_c^0 \left(1 - \frac{h_{cr}^{eff}}{h}\right)^{3/2}, \quad (4)
 \end{aligned}$$

where the bulk thermodynamic coercive field is $E_c^0 = \frac{2}{3\sqrt{3}} \sqrt{-\frac{\alpha^3}{\beta}}$ (for BFO, it is about 5×10^8 V/m) and $h_{cr}^{eff} = \frac{-d}{\alpha \varepsilon_0 \varepsilon_d}$ is the critical thickness for ferroelectricity. Using Eq. (4), we estimate the intrinsic thermodynamic switching bias as

$$U_c = E_c^b h \sim h \left(1 - \frac{h_{cr}^{eff}}{h}\right)^{3/2}. \quad (5)$$

At the same time, the values for spontaneous polarization are given by

$$\begin{aligned}
 P_z(E_b = 0, U = 0) &= \pm \sqrt{-\frac{\alpha_R}{\beta}} = \pm P_S^b \sqrt{1 + \frac{1}{\alpha \varepsilon_0} \frac{d}{\varepsilon_d h + \varepsilon_h^b d}} \\
 &\stackrel{\varepsilon_d h \gg \varepsilon_h^b d}{\approx} \pm P_S^b \sqrt{1 - \frac{h_{cr}^{eff}}{h}}, \quad (6)
 \end{aligned}$$

where the bulk spontaneous polarization is $P_S^b = \sqrt{-\frac{\alpha}{\beta}}$.

Within the Landau-Ginzburg-Devonshire approach, the out-of-plane strain u_{zz} and piezoresponse u_z of a tetragonal film are

$$\begin{aligned}
 u_{zz} &= \varepsilon_{33}^f \varepsilon_0 Q_{11} P_z E_z, \\
 u_z &\approx \int_0^h \varepsilon_{33}^f \varepsilon_0 Q_{11} P_z E_z dz \\
 &\sim \varepsilon_0 Q_{11} \frac{\varepsilon_{33}^0 h}{1 - h_{cr}^{eff}/h} \frac{U \varepsilon_d}{\varepsilon_d h + \varepsilon_h d} P_S^b \sqrt{1 - \frac{h_{cr}^{eff}}{h}} \\
 &\sim \frac{U}{\sqrt{1 - h_{cr}^{eff}/h}}. \quad (7)
 \end{aligned}$$

Under the assumption of constant dielectric permittivity ε_{33}^f , the piezoresponse is given by

$$u_z = U \sqrt{1 - \frac{h_{cr}^{eff}}{h}}. \quad (8)$$

Equation (8) can fit the experimentally observed thickness dependence of piezoresponse reasonably well, as seen in Fig. 4(a). The corresponding critical thickness h_{cr}^{eff} lies in the range from 1 to 2 nm, which is consistent with our observation of ferroelectric switching in BFO down to at least 1.6 nm. Using the bulk value for α ($\alpha = -8 \times 10^8$ m/F) and assuming ε_d between 1 and 4, the corresponding thickness of the dead layers is between 0.01 and 0.03 nm. Therefore, the dielectric gaps are very thin in this case, and the scaling mainly arises from the effect of the depolarizing field on the spontaneous polarization, rather than the electrostatic attenuation of the applied electric field inside the ferroelectric volume.

Equation (5) predicts that the nucleation bias scales linearly with the film thickness, deviating from linearity only when the thickness approaches the critical value h_{cr}^{eff} . The slope equals

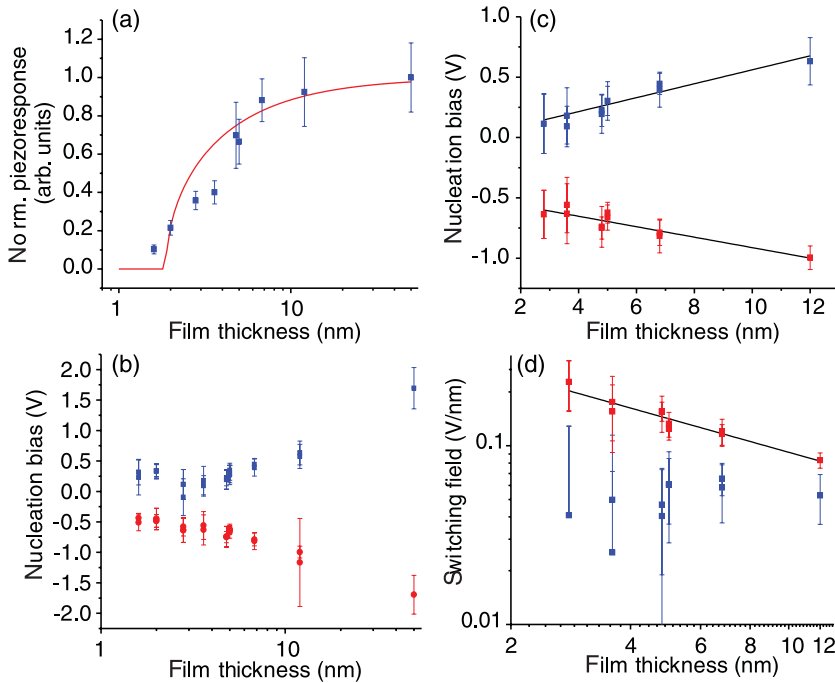


FIG. 4. (Color online) Thickness dependence of piezoresponse (medium gray/red) predicted by the intrinsic model, Eq. (8), with the assumption of a thickness-independent background dielectric constant ϵ_{33}^f and $h_{cr}^{eff} = 1.88$ nm. Dark gray (blue) dots are experimentally measured piezoresponse values from Fig. 3(a). Both theoretical and experimental values have been normalized to the piezoresponse at 50 nm. (b) Positive (blue squares) and negative (red circles) switching bias as a function of film thickness determined from the hysteresis loops. (c) Linear fitting of the average nucleation bias values for films in the thickness range between 2.8 and 12 nm. (d) Scaling of the apparent switching electric field (calculated as U_c/h), with film thickness for the positive (dark gray/blue) and negative (medium gray/red) polarity.

the coercive field in the bulk, or the region of the film far from the interfaces. As seen in Figs. 4(b) and 4(c), the experimental thickness dependencies of both positive and negative switching bias are indeed linear in almost all the measured range. The slopes are ~ 47 MV/m for the negative and ~ 58 MV/m for the positive switching bias. Assuming intrinsic switching and the bulk dielectric constant of $30\epsilon_0$,³³ these values correspond to a spontaneous polarization of ~ 25 $\mu\text{C}/\text{cm}^2$ in the (111) direction. This value is three- to fivefold smaller than the reported values for the BFO bulk,³³ but we consider the agreement to be satisfactory given the simplifying assumptions of our procedure and that polarization can be smaller in our particular thin films than the record values obtained for bulk or thick films of BFO.

A more significant disparity between theory and experiment is observed in the intercept of the magnitude of switching bias at zero thickness. According to Eq. (5), the maximum intercept is zero (at zero h_{cr}^{eff}). At nonzero critical thickness, switching bias becomes complex below h_{cr}^{eff} , formally translating into a negative intercept. The inspection of Fig. 4(c) reveals that (ignoring the two thinnest films) the scaling of the positive nucleation bias intercepts the y-axis at approximately zero, which is consistent with the very thin dielectric gaps estimated from the thickness dependence of piezoresponse. However, the values for the magnitude of the negative nucleation bias have a positive intercept.

Although at present we cannot explain the origin of the large intercept, it has a dramatic effect on the scaling of the apparent switching field, which is usually calculated as U_c/h (valid only in the limit of zero dielectric gap, as we discussed previously). Calculating the apparent switching field from our data [Fig. 4(d)] reveals that the positive switching field remains approximately constant across the thickness range, as expected based on the intrinsic switching model. However, because of a nonzero intercept the negative switching field scales approximately as $E_c \propto h^{-0.75 \pm 0.04}$, which is a similar trend

to the well-known Kay-Dunn law (coercive field $\propto h^{-0.66}$) derived for macroscopic films.¹⁸ The Kay-Dunn law should not apply for ultrathin films where the polarization nucleus becomes cylindrical.⁸ Furthermore, within the intrinsic model, the growth of the switching field with decreasing thickness implies an *increase* of spontaneous polarization, because as discussed previously, $|P_z| = \sqrt{-\frac{\alpha}{\beta}}$ and the coercive field $E_c^0 = \frac{2}{3\sqrt{3}}\sqrt{-\frac{\alpha^2}{\beta}}$ (α and β are the first and second coefficients in the Landau-Ginzburg-Devonshire equation of state). This would starkly contradict simultaneous piezoresponse measurements [Fig. 3(a)], which imply that polarization *decreases* with decreasing thickness. Piezoresponse measurements therefore provide sufficient self-consistency to rule out the rapid increase of the apparent switching field with decreasing film thickness.

C. Spatially resolved analysis of ferroelectric switching

Given the sensitivity of remnant piezoresponse to the properties of the dielectric gaps discussed in the previous sections, we anticipated some observable variation among local hysteresis loops across the surface. To verify this hypothesis, we acquired 9600 hysteresis loops on a grid of 80×40 points with a spatial resolution of 2 nm per pixel on the surface of the 2-nm BFO film. As seen in Fig. 5(a), systematic variations were indeed observable, with about twofold variation of piezoresponse magnitude across the surface, but well within the measurement accuracy. The changes were not all random, with piezoresponse on average smaller at the bottom and top of the map (light gray/green) and larger (medium gray/red) in the middle [Fig. 5(a)]. The pronounced regions of zero piezoresponse (dark gray/dark blue) in Fig. 5(a) correspond to defects on the surface where no hysteresis loop opening was observed. They are not discussed here further.

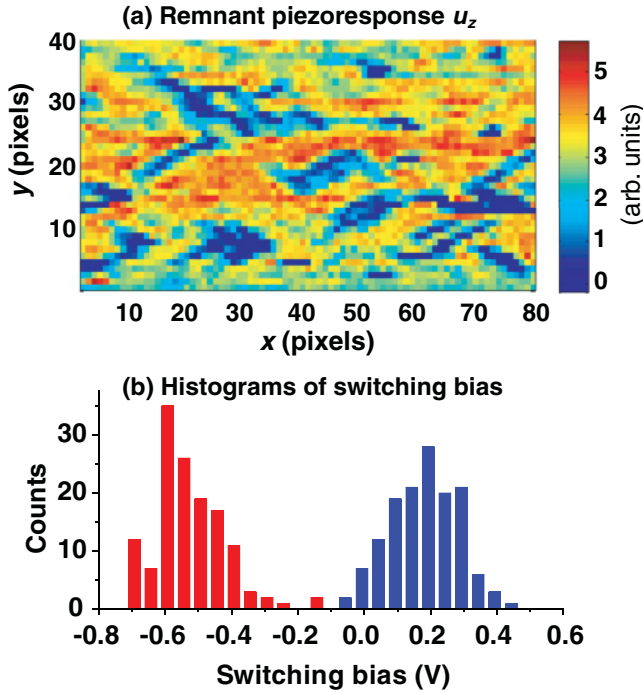


FIG. 5. (Color online) Spatially resolved hysteresis mapping of a 2-nm BFO film in ultrahigh vacuum. (a) The remnant piezoresponse extracted from an average of three hysteresis loops at each of the 3200 points of the map. The hysteresis loops did not open in the dark gray (dark blue) regions because of topographic defects. (b) Distributions of positive and negative switching bias across the surface of the 2-nm film.

The streakiness of some lines in Fig. 5(a) indicates abrupt changes between consecutive lines across the surface, which suggests that the changes in the critical thickness and the corresponding dielectric gaps are occurring at the top (Pt-BFO) rather than bottom (BFO-LSMO) interface. If we were to attribute the observed variations to subtle changes in the dielectric gap, the ratio of piezoresponse values from two locations on the surface would be $\frac{u_{z1}}{u_{z2}} = \sqrt{\frac{h-h_{cr1}^{eff}}{h-h_{cr2}^{eff}}}$. Although we do not have an independent measure of the respective critical thicknesses, for a 2-nm film, a twofold suppression of piezoresponse would be produced by increasing the critical thickness by a factor of 1.2 to 1.8 for the range of critical thicknesses from 1.6 to 1 nm (a range derived earlier and consistent with the film thickness range studied here).

Thus, piezoresponse mapping appears to be a sensitive probe of the local junction properties, particularly at the ultrathin limit. With increasing film thickness, the sensitivity of piezoresponse to the changes of the critical thickness diminishes. Prospectively, this trend can be used to differentiate local changes of the dielectric gap from surface-specific variations (e.g., contact potential difference and electrochemistry), which are present on the surface irrespective of film thickness. The extrinsic dead layer (which is likely going to be present in most measurements, particularly in ambient or liquids) does not impede ferroelectricity down to a length scale of the unit-cell. Furthermore, the absolute width of the distribution of the switching bias for ultrathin films is about ± 0.1 V [Fig. 5(b)], which is about an order of magnitude smaller

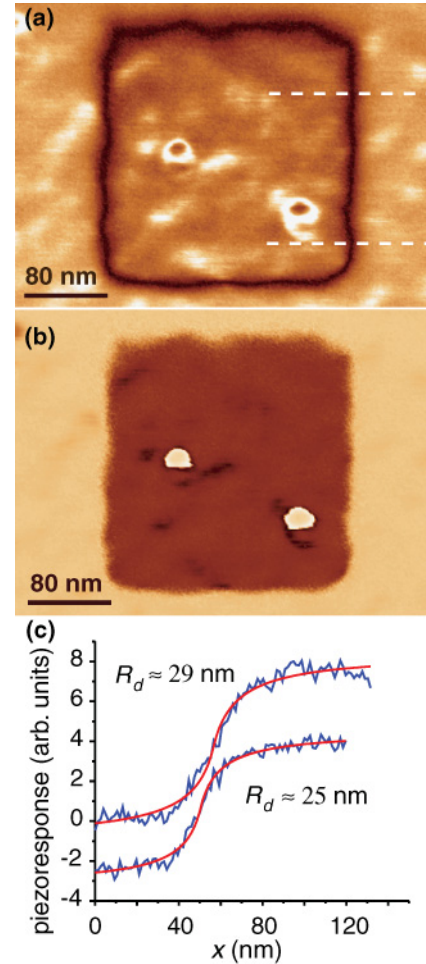


FIG. 6. (Color online) Estimating the effective tip size (tip modeled as a disc with radius R_d) using the width of a ferroelectric domain wall recorded on the surface of a 50-nm PbZrTiO₃ epitaxial film in ultrahigh vacuum. Images represent the recorded square domain in the amplitude (a) and phase (b) of piezoresponse. (c) The plot shows two domain wall profiles extracted approximately along the (white) dashed lines, and the corresponding fits following the procedure in the Appendix.

than that for 50-nm BFO films (± 1 V).²⁴ This has important practical implications for the reproducibility of devices based on nanoscale ferroelectrics.

IV. CONCLUSIONS

We have presented the first systematic and statistical analysis of the remnant piezoresponse hysteresis loops measured on a series of epitaxial thin films of BFO from 50 to 1.6 nm. All BFO films were found to be repeatedly and reproducibly switchable, demonstrating the feasibility of nanoscale ferroelectricity for the fundamental studies and device applications replying on polarization switching, such as polarization-controlled electron transport and ultrahigh density information storage.¹ Using the magnitude of piezoresponse to probe ferroelectricity, as well as the electrostatic properties of the ferroelectric junction, we have inferred that the shape of the ferroelectric hysteresis loop is primarily influenced by the

extrinsic dielectric gaps at the films' interfaces, which, in turn, suppress spontaneous polarization through the effect of the depolarizing field. An overall good agreement was obtained between the experimentally observed scaling of piezoresponse and switching field and the intrinsic model for ferroelectric switching. Thus, we have also been able to estimate the magnitude of spontaneous polarization in the studied films. However, the model cannot at present explain the offset in the switching bias for one of the switching polarities. This offset gives rise to a spurious Kay-Dunn-like scaling of the switching field. At the same time, the scaling is self-consistently ruled out by the corresponding scaling of piezoresponse.

Finally, we have demonstrated spatially resolved mapping of the extrinsic dielectric gap within nanometer-scale resolution based on the variations of individual ferroelectric hysteresis loops across the surface. The observed variations are consistent with our assignment of the imperfect tip-surface contact as the origin of the extrinsic dielectric gap. Such systematic measurements of nanoscale ferroelectricity now pose a possibility of exploring the scaling of the multiferroic properties of BFO down to a few unit cells in thickness. However, careful tip and surface preparation can prospectively eliminate the extrinsic dielectric gap and allow a more rigorous comparison between experiment and theory, including a possibility of increased piezoresponse with decreasing film thickness motivated by the intrinsic model.

ACKNOWLEDGMENTS

PFM experiments were carried out at the Center for Nanophase Materials Sciences, Division of User Facilities, US Department of Energy. The work was supported in part (S.V.K., H.J.C., A.Y.B.) by the Materials Sciences and Engineering Division, Basic Energy Sciences, US Department of Energy. The work at Berkeley is supported by the Director, Office of Science, Office of Basic Energy Sciences, Materials Sciences

Division of the US Department of Energy under Contract No. DE-AC02-05CH1123.

APPENDIX

To support our use of the 1D approximation for the electrostatics of the problem, we estimated the tip size based on the width of the domain wall profile as detailed in Ref. 34. Figure 6 shows the image of the poled domain structure on a reference 50-nm epitaxial film of $\text{PbZr}_{0.2}\text{Ti}_{0.8}\text{O}_3$ and line profiles of the corresponding domain walls. The domain wall profile was fitted using the following equation:³⁴

$$u(x) \approx u_0 + \alpha \left[\frac{3}{4} \left(d_{33} + \left(\frac{1}{3} + \frac{4}{3} \nu \right) d_{31} \right) \times \frac{(x - x_0)/r}{|(x - x_0)/r| + 1/4} + \frac{1}{4} d_{15} \frac{(x - x_0)/r}{|(x - x_0)/r| + 3/4} \right],$$

where $u(x)$ is the measured piezoresponse, d_{ij} are the piezoelectric coefficients, ν is the Poisson ratio. α is the proportionality coefficient, x_0 is the relative center of the domain wall, and $r = 2R_d/\pi$, where R_d is the disc radius, assuming a model of a disc and a single image charge description of the localized electric field, are all fitting parameters.³⁴ Based on the reasonably good fit (Fig. 6), the radius of the disc (approximating the AFM tip apex) equals 25 and 29 nm for the two walls, which is also in good agreement with the width of the domain walls (~ 29 and ~ 33 nm, respectively). Therefore, our typical effective tip size is much larger than the thickness of all ultrathin films (with the exception of the 50-nm BFO film, which is used only as a reference). Thus, the relatively large tip size justifies the use of the 1D approximation for the electric field in this study. Parenthetically, the effective tip size in ultrahigh vacuum is approximately twofold smaller than in the ambient environment.

*5nm@ornl.gov

¹E. Y. Tsymlal and H. Kohlstedt, *Science* **313**, 181 (2006).

²I. I. Naumov, L. Bellaiche, and H. X. Fu, *Nature* **432**, 737 (2004).

³L. Yu, V. Ranjan, M. B. Nardelli, and J. Bernholc, *Phys. Rev. B* **80**, 165432 (2009).

⁴M. Gajek, M. Bibes, S. Fusil, K. Bouzehouane, J. Fontcuberta, A. Barthélémy, and A. Fert, *Nat. Mater.* **6**, 296 (2007).

⁵J. P. Velev, C. Velev, J. D. Burton, A. Smogunov, M. K. Niranjan, E. Tosatti, S. S. Jaswal, and E. Y. Tsymlal, *Nano Lett.* **9**, 427 (2009).

⁶J. Junquera and P. Ghosez, *Nature* **422**, 506 (2003).

⁷V. Nagarajan, S. Prasertchoung, T. Zhao, H. Zheng, J. Ouyang, R. Ramesh, W. Tian, X. Q. Pan, D. M. Kim, C. B. Eom, H. Kohlstedt, and R. Waser, *Appl. Phys. Lett.* **84**, 5225 (2004).

⁸J. Y. Jo, Y. S. Kim, T. W. Noh, J. Yoon, and T. K. Song, *Appl. Phys. Lett.* **89**, 232909 (2006).

⁹A. N. Morozovska, E. A. Eliseev, Y. Li, S. V. Svechnikov, P. Maksymovych, V. Y. Shur, V. Gopalan, L. Q. Chen, and S. V. Kalinin, *Phys. Rev. B* **80**, 214110 (2009).

¹⁰S. Ducharme, V. M. Fridkin, A. V. Bune, S. P. Palto, L. M. Blinov, N. N. Petukhova, and S. G. Yudin, *Phys. Rev. Lett.* **84**, 175 (2000).

¹¹M. Dawber, P. Chandra, P. Littlewood, and J. Scott, *J. Phys. Condens. Matter* **15**, L393 (2003).

¹²G. Catalan, H. Béa, S. Fusil, M. Bibes, P. Paruch, A. Barthélémy, and J. F. Scott, *Phys. Rev. Lett.* **100**, 027602 (2008).

¹³D. D. Fong, G. Stephenson, S. Streiffer, J. A. Eastman, O. Auciello, P. H. Fuoss, and C. Thompson, *Science* **304**, 1650 (2004).

¹⁴S. H. Baek, H. W. Jang, C. M. Folkman, Y. L. Li, B. Winchester, J. X. Zhang, Q. He, Y. H. Chu, C. T. Nelson, M. S. Rzchowski, X. Q. Pan, R. Ramesh, L. Q. Chen, and C. B. Eom, *Nat. Mater.* **9**, 309 (2010).

¹⁵J. E. Spanier, A. M. Kolpak, J. J. Urban, I. Grinberg, L. Ouyang, W. S. Yun, A. M. Rappe, and H. Park, *Nano Lett.* **6**, 735 (2006).

¹⁶M. Dawber, K. M. Rabe, and J. Scott, *Rev. Mod. Phys.* **77**, 1083 (2005).

¹⁷T. Shaw, S. Trolrier-McKinstry, and P. McIntyre, *Ann. Rev. Mater. Sci.* **30**, 263 (2000).

¹⁸H. F. Kay and J. W. Dunn, *Philos. Mag.* **7**, 2027 (1962).

¹⁹R. Landauer, *J. Appl. Phys.* **28**, 227 (1957).

²⁰A. M. Bratkovsky and A. P. Levanyuk, *J. Comp. Theor. Nanosci.* **6**, 465 (2009).

- ²¹S. V. Kalinin, B. J. Rodriguez, S. Jesse, P. Maksymovych, K. Seal, M. Nikiforov, A. P. Baddorf, A. L. Kholkin, and R. Proksch, *Mat. Today* **11**, 16 (2008).
- ²²Y. H. Chu, T. Zhao, M. P. Cruz, Q. Zhan, P. L. Yang, L. W. Martin, C. H. Yang, F. Zavaliche, H. Zheng, and R. Ramesh, *Appl. Phys. Lett.* **90**, 252906 (2007).
- ²³M. Huijben, L. W. Martin, Y.-H. Chu, M. B. Holcomb, P. Yu, G. Rijnders, D. H. A. Blank, and R. Ramesh, *Phys. Rev. B* **78**, 094413 (2008).
- ²⁴P. Maksymovych, S. Jesse, M. Huijben, R. Ramesh, A. Morozovska, S. Choudhury, L. Q. Chen, A. P. Baddorf, and S. V. Kalinin, *Phys. Rev. Lett.* **102**, 017601 (2009).
- ²⁵S. Jesse, P. Maksymovych, and S. V. Kalinin, *Appl. Phys. Lett.* **93**, 112903 (2008).
- ²⁶A. N. Morozovska, E. A. Eliseev, S. V. Svechnikov, A. D. Krutov, V. Y. Shur, A. Y. Borisevich, P. Maksymovych, and S. V. Kalinin, *Phys. Rev. B* **81**, 205308 (2010).
- ²⁷D. D. Fong, A. M. Kolpak, J. A. Eastman, S. K. Streiffer, P. H. Fuoss, G. B. Stephenson, C. Thompson, D. M. Kim, K. J. Choi, C. B. Eom, I. Grinberg, and A. M. Rappe, *Phys. Rev. Lett.* **96**, 127601, (2006).
- ²⁸H. Béa, S. Fusil, K. Bouzehouane, M. Bibes, M. Sirena, G. Herranz, E. Jacquet, J. Contour, and A. Barthélémy, *Jpn. J. Appl. Phys.* **45**, L187 (2006).
- ²⁹T. Tybell, C. Ahn, and J. Triscone, *Appl. Phys. Lett.* **75**, 856 (1999).
- ³⁰H. Fujisawa, M. Okaniwa, H. Nonomura, M. Shimizu, and H. Nlu, *J. Eur. Ceram. Soc.* **24**, 1641 (2004).
- ³¹Y. Xie, C. Bell, T. Yajima, Y. Hikita, and H. Y. Hwang, *Nano Lett.* **10**, 2588 (2010).
- ³²S. V. Kalinin, B. J. Rodriguez, S. Jesse, Y. H. Chu, T. Zhao, R. Ramesh, S. Choudhury, L. Chen, E. A. Eliseev, and A. N. Morozovska, *PNAS* **104**, 20204 (2007).
- ³³G. Catalan and J. F. Scott, *Adv. Mater.* **21**, 2463 (2009).
- ³⁴S. V. Kalinin, S. Jesse, B. J. Rodriguez, E. A. Eliseev, V. Gopalan, and A. N. Morozovska, *Appl. Phys. Lett.* **90**, 212905 (2007).